

AD-A157 479

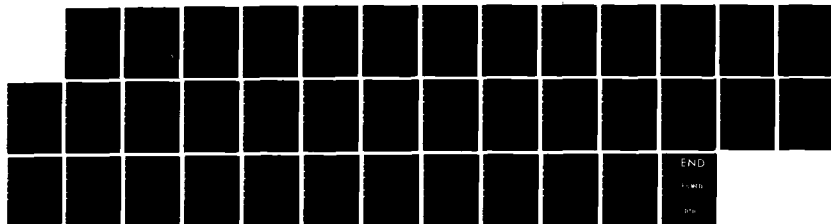
NONEQUILIBRIUM ELECTRONIC POLARIZATION OF THE SOLVENT  
IN PHOTOIONIZATION(U) NEW YORK UNIV NY DEPT OF  
CHEMISTRY P DELAHAY ET AL JUL 85

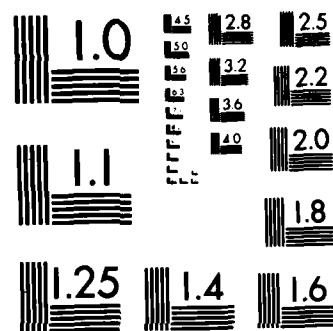
1/1

UNCLASSIFIED

NYU/DC/TR-8-NEW-SERIES-2 N00014-82-K-0113 F/G 7/4

NL





MICROCOPY RESOLUTION TEST CHART  
NBS-1963-A

2

AD-A157 479

OFFICE OF NAVAL RESEARCH

Contract N00014-K-0113

Task No. NR 359-258

TECHNICAL REPORT NO. NYU/DC/TR-8-NEW-SERIES-2

NONEQUILIBRIUM ELECTRONIC POLARIZATION  
OF THE SOLVENT IN PHOTOIONIZATION

by

Paul Delahay and Andrew Dziedzic

Submitted for publication in  
Journal of Chemical Physics

New York University  
Department of Chemistry  
New York, NY

July 1985

DTIC  
ELECTE  
AUG 07 1985  
S E D

DTIC FILE COPY

Reproduction in whole or in part is permitted for  
any purpose of the United States Government

This document has been approved for public release  
and sale; its distribution is unlimited

85 8 1 095

**SECURITY CLASSIFICATION OF THIS PAGE (When Data Entered)**

DD FORM 1473  
1 JAN 73

Unclassified

**SECURITY CLASSIFICATION OF THIS PAGE (When Data Entered)**

20.

the energetics of photoionization are calculated for transparent and absorbing solvents: electronic polarization, London dispersion and Born repulsion energies for a discrete model of coordinated solvent molecules in the inner-sphere solvation shell of anions and cations; electronic polarization of the outer-sphere region for a continuous medium model. The losses resulting from the rapid variation of the ionic field for an absorbing solvent are calculated for the inner- and outer-sphere regions, respectively, from a discrete model and a continuous medium. Damping of the ionic field resulting from solvent absorption is negligible. The theory is applied to aqueous solutions in the 7 to 10.4 eV range of photon energies by using dielectric data from reflectance spectroscopy of liquid water. Experimental dispersion spectra for photoelectron emission have the shape predicted by theory and display all the extrema at the photon energies of the calculated curves. The very pronounced effect of ionic strength on the balance between inner- and outer-sphere contributions predicted by theory (inner-outer sphere splitting) is fully confirmed by experiment. Dispersion spectra of inorganic ions in the range of each of the two absorption bands of liquid water (maxima at ca. 8.2 and 10.0 eV) therefore exhibit a double maximum for normal dispersion and a double minimum for anomalous dispersion (12 extrema between 7.2 and 10.4 eV). Specific effect of the nature of anions is evident above 9.0 eV in inner-outer sphere splitting. The present study provides a way of probing the response of liquids and solutions to the rapidly varying intense ionic field resulting from the process of photoionization.

|                    |                                     |  |
|--------------------|-------------------------------------|--|
| Accession For      |                                     |  |
| NTIS GRA&I         | <input checked="" type="checkbox"/> |  |
| DTIC TAB           | <input type="checkbox"/>            |  |
| Unannounced        | <input type="checkbox"/>            |  |
| Justification      |                                     |  |
| By                 |                                     |  |
| Distribution/      |                                     |  |
| Availability Codes |                                     |  |
| All and/or         |                                     |  |
| Dist               | Special                             |  |
| A-1                |                                     |  |

# Nonequilibrium electronic polarization of the solvent in photoionization

Paul Delahay and Andrew Dziedzic

Department of Chemistry, New York University, New York, New York 10003

(Received

)

The energetics of photoionization in condensed phases includes a significant contribution from nonequilibrium processes arising from dielectric dispersion of the solvent at the prevailing photon energy. The solvent is polarized by the varying electric field caused by the change of ionic valence as a result of photoionization. This ionic field varies in a time interval determined by the frequency of incident radiation. The following contributions from nonequilibrium processes to the energetics of photoionization are calculated for transparent and absorbing solvents: electronic polarization, London dispersion and Born repulsion energies for a discrete model of coordinated solvent molecules in the inner-sphere solvation shell of anions and cations; electronic polarization of the outer-sphere region for a continuous medium model. The losses resulting from the rapid variation of the ionic field for an absorbing solvent are calculated for the inner- and outer-sphere regions, respectively, from a discrete model and a continuous medium. Damping of the ionic field resulting from solvent absorption is negligible. The theory is applied to aqueous solutions in the 7 to 10.4 eV range of photon energies by using dielectric data from reflectance spectroscopy of liquid water. Experimental dispersion spectra for photoelectron emission have the shape predicted by theory and display all the extrema at the photon energies of the calculated curves. The very pronounced effect of ionic strength on the balance between inner- and outer-sphere contributions predicted by theory (inner-outer sphere splitting) is fully confirmed by experiment. Dispersion spectra of inorganic ions in the range of

each of the two absorption bands of liquid water (maxima at ca. 8.2 and 10.0 eV) therefore exhibit a double maximum for normal dispersion and a double minimum for anomalous dispersion (12 extrema between 7.2 and 10.4 eV). Specific effect of the nature of anions is evident above 9.0 eV in inner-outer sphere splitting. The present study provides a way of probing the response of liquids and solutions to the rapidly varying intense ionic field resulting from the process of photoionization.

## I. INTRODUCTION

Dielectric dispersion of the solvent was shown recently<sup>1</sup> to affect the energetics of photoionization of ions and molecules in solution. This effect was interpreted<sup>1,2</sup> by assuming that the energetics of solvation of the species being photoionized is determined by the solvent polarizability  $\alpha$  and optical dielectric constant  $\epsilon_{op}$  at the photon energy  $E$  at which photoionization occurs rather than by the limiting value  $\alpha^0$  and  $\epsilon_{op}^0$ . Alternatively, one may assume that the change of ionic valence of the substance being photoionized occurs on a time scale determined by the frequency of the incident radiation. The response of the medium to the rapidly varying intense ionic field is determined under these conditions by  $\alpha$  and  $\epsilon_{op}$  at the photon energy  $E$  and not by the limiting values  $\alpha^0$  and  $\epsilon_{op}^0$ . The dispersion effect according to this model results from nonequilibrium processes involving electronic polarization of the solvent, London dispersion and Born repulsion. Energy losses resulting from the rapid variations of the ionic field must also be considered for absorbing solvents. This model is treated quantitatively and tested experimentally in the present paper. Differences in the solvent configuration around anions and cations are taken into account following a comment by Hush<sup>3</sup> on the earlier treatment.

The selection of the proper dielectric constant of the solvent in the present treatment follows from the three-step model<sup>4</sup> used in the interpretation of photoelectron emission by liquids<sup>5,6</sup>: (i) photoionization, (ii) transfer of quasifree electrons to the liquid-gas interface, and (iii) interfacial barrier problem. Dispersion affects only photoionization, and the dielectric constant  $\epsilon_{op}$  is selected accordingly, as noted above. The proper dielectric constant (or range of dielectric constants) in the ion-electron separation of the above step (ii) is determined by the kinetic energy of the quasifree electrons generated by photoionization. The present paper is not concerned with this problem since ion-electron separation and transfer are embodied in the emission law accounted, for instance, by the theory of Refs. 5 and 6.

## II. NONEQUILIBRIUM PROCESSES: TRANSPARENT SOLVENTS

### A. Theoretical model

The fairly standard treatment of ionic solvation<sup>7,8</sup> will be adapted to the present problem with the additional consideration of the different solvent configurations around inorganic anions and cations. Electrically neutral species can be treated in terms of the continuous medium model of Sec. IIC without any particular difficulty. The volume around the ion being photoionized is divided into two regions. (i) The inner-sphere solvation shell consists of  $N$  solvent molecules coordinated to the ion. The solvent molecules are treated as point dipoles at a distance  $r_o = r_c + r_w$  from the ionic charge, where  $r_c$  and  $r_w$  are the crystallographic radii of the ion and solvent, respectively. (ii) The outer-sphere region outside the sphere of radius  $a = r_c + 2r_w$  is treated as a continuous medium.



The nonequilibrium contribution from electronic polarization in the present treatment is determined by the change  $\Delta z = 1$  in the ionic valence and thus is independent of the value of  $z$  as in the case of nuclear reorganization of the outer-sphere region (Marcus,<sup>9</sup> Hush<sup>10</sup>). A multipole expansion<sup>11</sup> of the potential of the ion will be used as in the calculation of energies of ionic solvation. The polarizability of the solvent is assumed to be isotropic. This is nearly the case for water considered below in the application of the theory. Calculated energies differ by only ca. 1 percent if anisotropy is taken into account on the basis of the polarizability data of Ref. 12. The induced dipole vector is collinear with the electric field vector in the central field of the ionic charge if one assumes isotropic polarizability of the solvent. Nonlinear effects are not considered.

#### B. Inner-sphere solvation shell

Only the terms depending on  $\alpha$  and  $\epsilon_{op}$  of the solvent and the terms for London dispersion and Born repulsion are retained in the expression for the free energy of ionic solvation.<sup>7,8</sup> We calculate first the change of energy  $\Delta P_{in}$  for the inner-sphere solvation shell for  $\Delta z = 1$  and the change of polarizability from  $\alpha$  to  $\alpha^0$ . One has

$$\begin{aligned} \Delta P_{in} = & \Delta U_{IND} + \Delta U(p_{\alpha}e) + \Delta U(p_{\alpha}p) + \Delta U(p_{\alpha}p_{\alpha}) + \Delta U(p_{\alpha}q) \\ & + \Delta U_L(S,s) + \Delta U_L(s,s) + \Delta U_{REP}, \end{aligned} \quad (1)$$

where  $U_{IND}$  represents the work required for the formation of induced dipoles  $p_{\alpha}$  in the inner-sphere solvation shell; the next four terms are the energies of interaction of induced dipoles with the ionic charge ( $p_{\alpha}e$ ), dipoles ( $p_{\alpha}p$ ), induced dipoles ( $p_{\alpha}p_{\alpha}$ ), quadrupoles ( $p_{\alpha}q$ );  $U_L(S,s)$  and  $U_L(s,s)$  are the energies for solute-solvent and solvent-solvent London dispersion, respectively;  $U_{REP}$  corresponds to solute-solvent and solvent-solvent Born repulsion.

Explicit forms are:

$$\Delta U_{IND} = (N/2)[(p_{\alpha}^0)^2/\alpha^0 - p_{\alpha}^2/\alpha] \quad (2)$$

$$\Delta U(p_{\alpha}e) = - (Ne/r_0^2)(p_{\alpha}^0 - p_{\alpha}) \quad (3)$$

$$\Delta U(p_{\alpha}p) = 2A(p/r_0^3)(p_{\alpha}^0 - p_{\alpha})\cos \beta \quad (4)$$

$$\Delta U(p_{\alpha}p_{\alpha}) = (A/r_0^3)[(p_{\alpha}^0)^2 - p_{\alpha}^2] \quad (5)$$

$$\Delta U(p_{\alpha}q) = - B(\Theta/r_0^4)(p_{\alpha}^0 - p_{\alpha}) \quad (6)$$

$$\Delta U_L(S,s) = - (3N/2r_0^6)[I_s I/(I_s + I)]\alpha_s(\alpha^0 - \alpha) \quad (7)$$

$$\Delta U_L(s,s) = - (CI/r_0^6)[(\alpha^0)^2 - \alpha^2] \quad (8)$$

$$\Delta U_{REP} = - (1/x)\{2\Delta U(p_{\alpha}e) + 3[\Delta U(p_{\alpha}p) + \Delta U(p_{\alpha}p_{\alpha})] + 4\Delta U(p_{\alpha}q) + 6[\Delta U_L(S,s) + \Delta U_L(s,s)]\} \quad (9)$$

where  $N$  is the number of solvent molecules coordinated to the species being photoionized;  $e$ , the absolute value of the electronic charge;  $p$ , the permanent dipole moment of the solvent;  $\Theta$ , the quadrupole moment of the solvent (Appendix);  $\beta$ , the angle between the induced and permanent dipoles of the solvent in the inner-sphere solvation shell;  $I_s$  and  $I$ , the gas-phase ionization energies of the solute and solvent, respectively;  $\alpha_s$ , the polarizability of the solute taken to be independent of photon energy in the absence of dispersion data. The coefficients  $A$ ,  $B$  and  $C$  were calculated by Buckingham<sup>7</sup> by considering solvent pairwise interactions:  $A = 2.296$  and  $7.114$ ;  $B = 1.722$  and  $5.336$ ;  $C = 0.2373$  and  $1.160$  for tetrahedral and octahedral coordination, respectively. The Born repulsion energy  $U_{REP}$  is obtained according to Morf and Simon<sup>8</sup> by minimizing with respect to  $r_0$  the total contribution from the inner-sphere shell to the solvation energy. The exponent  $x$  will be taken to be 12 and 8, respectively, for inorganic anions<sup>13</sup> and cations.<sup>8</sup>

The induced dipole moment  $p_{\alpha}^0$  is obtained according to Morf and Simon<sup>8</sup> by minimizing with respect to  $p_{\alpha}^0$  the total energy depending on  $p_{\alpha}^0$ . Thus,

$$p_{\alpha}^0 = \alpha^0 (Ner_0^2 - 2Apr_0 \cos \beta + B\theta) / r_0 (Nr_0^3 + 2A\alpha^0) \quad (10)$$

The same equation with  $\alpha$  instead of  $\alpha^0$  is applied to  $p_{\alpha}$ . Equation (10) reduces to the familiar equation  $p_{\alpha}^0 = \alpha^0 F$ , where  $F = e/r_0^2$  is the field, if the pairwise interactions are neglected.<sup>14</sup> The sum of the energies in Eqs. (2) and (3) in that case is one-half of the value on the r.h.s. of Eq. (3).

The evaluation of the angle  $\beta$  in Eq. (4) and  $\theta$  (Appendix A) requires information about the structure of the solvent in the inner-sphere shell. Only inorganic anions and cations in aqueous solution will be considered here. The anion, hydrogen and oxygen are collinear in the simplest case<sup>15-17</sup> and the water dipole vector makes an angle  $\beta = 52.23^\circ$  with the electric field vector of the ionic charge. The water molecules are assumed to rotate freely about the anion-hydrogen-oxygen axis.<sup>13</sup> Conversely, the cation and water molecule are assumed to be in the same plane in the simplest case with the cation-oxygen axis coinciding with the electric field vector of the ionic charge<sup>15-17</sup> ( $\beta = 0$ ). The water molecule is assumed to rotate freely about the cation-oxygen axis.<sup>7</sup> Tilting of the plane of the water molecule with respect to the cation-oxygen axis, which was reported<sup>15-17</sup> for high electrolyte concentrations ( $> 1.5$  M), will not be considered here but could easily be introduced in the treatment. To summarize, the limiting values  $\beta = 52.23^\circ$  and  $\beta = 0$  will be used for anions and cations, respectively, in the application of the theory to aqueous solutions.

### C. Screening by the ionic atmosphere

The change in the free energy for electronic polarization of the outer-sphere region is treated for a continuous-medium model. One has

$$\Delta P_{\text{out}} = (e^2/2a)[(\epsilon_{\text{op}}^0)^{-1} - \epsilon_{\text{op}}^{-1}] \quad (11)$$

in the absence of screening of the ions by the ionic atmosphere. A correction must be made for the screening. The free energy contribution  $\Delta G_{\text{atm}}$  from the ionic atmosphere to the free energy of electronic polarization of the outer-sphere region is,

$$\Delta G_{\text{atm}} = - (e^2/2\epsilon_{\text{op}})\kappa/(1 + \kappa a), \quad (12)$$

to the approximation of the Debye-Hückel theory. There  $\epsilon_{\text{op}}$  is the optical dielectric constant,  $a$  is the radius of the inner-sphere taken to be equal to  $r_c + r_w$  (Sec. IIA), and  $\kappa$  is the Debye-Hückel reciprocal length measured from a. The quantity  $\kappa$  is calculated for the static dielectric constant  $\epsilon_s$  of the solvent because the ionic atmosphere is "frozen" during the rapid variations of the ionic field resulting from photoionization. Equation (12) is taken directly from the Debye-Hückel theory<sup>18</sup> except that  $\epsilon_{\text{op}}$  is written in the denominator instead of  $\epsilon_s$ . A correction identical to Eq. (12) applies to nuclear reorganization<sup>19</sup> in optical electron transfer except that  $\epsilon_s$  appears in the denominator instead of  $\epsilon_{\text{op}}$ .

It is seen from Eq. (12) that the correction for the ionic atmosphere is obtained by writing  $(e^2/2R)(1/\epsilon_{\text{op}})$  with a radius  $R = a + 1/\kappa$  instead of  $R = a$ . The energy  $S\Delta P_{\text{out}}$  therefore is obtained instead of  $\Delta P_{\text{out}}$  of Eq. (11), the screening factor being,

$$\begin{aligned} S &= [a^{-1} - (a + 1/\kappa)^{-1}]/a^{-1} \\ &= 1/(1 + \kappa a). \end{aligned} \quad (13)$$

Thus, the value  $S = 1$  corresponds to the limiting case of no screening approximated for very dilute solutions. Conversely, the value  $S = 0$  pertains

to total screening of the outer-sphere response. One has, for instance, for a 0.1 M aqueous solution of a 1-1 electrolyte,  $\kappa^{-1} \sim 6.9 \text{ \AA}$  denoting the thickness of the ionic atmosphere outside the inner-sphere of radius  $a = 4.76 \text{ \AA}$ ; consequently,  $S \approx 0.6$ . Thus, the effect of screening by the ionic atmosphere in aqueous solutions can be very significant for electronic polarization whereas it is minor for nuclear reorganization in optical electron transfer (a few hundredths of electronvolt at most for a concentrated solution).

Expressions for the ionic screening of the discrete inner-sphere are complicated but may be closely approximated by a simple extension of the continuum outer-sphere treatment. For solutions of high ionic strength, counterions may penetrate the inner-sphere; thus, the Debye-Hückel length  $\kappa^{-1}$ , measured from the radius  $a$ , is negative denoting this penetration. The screening factor  $S$  is then negative allowing for the partial cancellation of the inner-sphere response by that calculated for the screened outer-sphere (see Sec. IV). For example, in a 2 M aqueous solution of a 2-1 electrolyte, the mean separation of ionic centers is  $\sim 6.5 \text{ \AA}$ . Given an effective common ionic radius<sup>18</sup>  $r_c \approx 2 \text{ \AA}$ , the distance from one of the ions to the center of the other is  $4.5 \text{ \AA}$ . Thus, the inner-sphere is penetrated to a depth of  $4.76 - 4.50 = 0.26 \text{ \AA}$ .  $\kappa^{-1}$  as defined above is then  $\approx -0.3 \text{ \AA}$  and consequently  $S$  is ca.  $-0.1$ .

Formula (13) is intended as a guide in the interpretation of screening rather than a quantitative equation. Application of the Debye-Hückel theory outside the range of sufficiently dilute solutions is tentative, but the original model can be improved (e.g., the recent treatment in Ref. 20). It is noted, in this respect, that departure from the theory does not arise because  $\kappa^{-1}$  in concentrated solutions is shorter than ionic radii since the ionic

atmosphere is always outside the sphere of closest approach for the ions the radius of which is approximately the sum of the anionic and cationic radii.

### III. NONEQUILIBRIUM PROCESSES: ABSORBING SOLVENTS

#### A. Real part of energies for inner- and outer-sphere regions

The dielectric constant of the solvent in the range of absorption is a complex quantity  $\epsilon_1 - i\epsilon_2$ . The energy density within the dielectric is  $\epsilon_1 F^2/8\pi$ , where  $F = (e/r^2)(\epsilon_1^2 + \epsilon_2^2)^{-1/2}$  is the magnitude of the ionic field. Integrating the energy density for the volume element  $dV = 4\pi r^2 dr$  between  $r = a$  and  $r = \infty$ , one obtains the outer-sphere contribution

$$\Delta P_{\text{out}} = (e^2/2a)[(\epsilon_{\text{op}}^0)^{-1} - \epsilon_1/(\epsilon_1^2 + \epsilon_2^2)]. \quad (14)$$

Thus, Eq. (14) is simply the real part of  $\Delta P_{\text{out}}$  of Eq. (11) written for a complex dielectric constant.

Similarly, calculation of  $\Delta P_{\text{in}}$  requires the value of the real part  $\alpha_1$  of the complex polarizability  $\alpha_1 - i\alpha_2$ . The values of  $\alpha_1$  and  $\alpha_2$  are obtained, at least approximately, from the Lorenz-Lorentz equation for an absorbing solvent<sup>21</sup>

$$(\epsilon_1 - 1 - i\epsilon_2)/(\epsilon_1 + 2 - i\epsilon_2) = \zeta(\alpha_1 - i\alpha_2), \quad (15)$$

where  $\zeta = 4\pi N_A \delta/3M$ ,  $N_A$  being the Avogadro number,  $\delta$  the density and  $M$  the molecular weight of the solvent. Equation (15) yields

$$[(\epsilon_1 - 1)(\epsilon_1 + 2) + \epsilon_2^2]/[(\epsilon_1 + 2)^2 + \epsilon_2^2] = \zeta\alpha_1 \quad (16)$$

$$\epsilon_2/[(\epsilon_1 + 2)^2 + \epsilon_2^2] = (\zeta/3)\alpha_2 \quad (17)$$

The energy  $\Delta P_{\text{in}}$  is computed from Eqs. (1) to (9) by using  $\alpha_1$  from Eq. (16) instead of  $\alpha$ . Equations (2) to (6) are written in complex form in terms of  $\alpha_1 - i\alpha_2$  and  $p_{\alpha_1} - ip_{\alpha_2}$  (Sec. IIIB). The sum of these complex energies is minimized with respect to  $p_{\alpha_1} - ip_{\alpha_2}$ , and the real and

imaginary parts of induced dipole are obtained accordingly. Thus,

$$p_{\alpha_1} = [K_1 K_3 (\alpha_1^2 + \alpha_2^2) + K_1 K_2 \alpha_1] / (K_2 + K_3 \alpha_1)^2 + (K_3 \alpha_2)^2 \quad (18)$$

$$p_{\alpha_2} = \alpha_2 K_1 K_2 / [(K_2 + K_3 \alpha_1)^2 + (K_3 \alpha_2)^2] \quad (19)$$

where

$$K_1 = N e r_0^2 = 2 A \rho r_0 \cos \beta + B \quad (20)$$

$$K_2 = N r_0^4 \quad (21)$$

$$K_3 = 2 A r_0 \quad (22)$$

Use of the corrected Lorenz-Lorentz equation<sup>21</sup> yielded values of  $\alpha_1$  and  $\alpha_2$  slightly higher than those given by Eqs. (16) and (17) (cf. also Sec. V).

#### B. Imaginary part of energies for inner- and outer-sphere regions

The imaginary part  $\epsilon_2$  of the complex dielectric constant can be interpreted classically in terms of the optical conductivity  $\sigma = \omega \epsilon_2 / 4\pi$  at the photon energy  $\hbar\omega$ . This interpretation holds even if the dielectric does not exhibit any conductivity from free charges, and the imaginary part  $\epsilon_2$  arises solely from bound-bound transitions. (The contribution from ionic conductivity for the systems studied in the present work is negligible.) The energy loss corresponding to absorption will be calculated for the outer- and inner-sphere regions. The loss for the outer-sphere region will be calculated first since a continuous medium treatment is directly applicable.

The conduction current density for the field  $F$  is  $\sigma F$ . The corresponding energy loss in the dielectric is determined by the variation of  $F$  during the time interval for which the loss is calculated. This time interval is taken to be equal to the time uncertainty  $\omega^{-1}$  corresponding to the photon energy  $E = \hbar\omega$  at which photoionization occurs. (See formulation of the time-energy uncertainty in Ref. 22.) The ionic valence cannot be specified during the

interval  $\omega^{-1}$  and consequently the loss is calculated by equating  $F$  to the change in ionic field from an ionic charge  $z$  to  $z + 1$  as a result of photoionization. The loss per unit of time and unit volume therefore is  $\sigma F^2$ . This result differs from the classical value<sup>21</sup>  $\sigma F^2/2$  obtained from  $\int_0^F \sigma E dE$ . The experimental results on the effect of ionic atmosphere in Sec. VI strongly support the use of  $\sigma F^2$  instead of  $\sigma F^2/2$ .

The energy loss per unit volume in the time  $\omega^{-1}$  is  $\omega^{-1}\sigma F^2$  or  $(\epsilon_2/4\pi)F^2$ . The ionic field in the absence of screening by the ionic atmosphere is  $(e/r^2)(\epsilon_1^2 + \epsilon_2^2)^{-1/2}$ , and the volume element  $dV$  is  $4\pi r^2 dr$ . The energy loss in the outer-sphere region is

$$\begin{aligned} L_{\text{out}} &= \epsilon_2 \int_a^{\infty} F^2 r^2 dr \\ &= (e^2/a)\epsilon_2/(\epsilon_1^2 + \epsilon_2^2). \end{aligned} \quad (23)$$

Equation (23) is identical, except for the factor  $1/2$ , to the negative imaginary part of the complex polarization which is associated with the real part of the polarization given by Eq. (14). The correction for the ionic atmosphere is obtained just as in Sec. IIC by introducing the radius  $a + 1/\kappa$  instead of  $a$  in Eq. (23). The screening factor  $S$  of Eq. (13) therefore is also applicable to  $L_{\text{out}}$ .

The loss in the inner-sphere  $L_{\text{in}}$  is calculated analogously to  $L_{\text{out}}$  by summing the negative imaginary parts of the complex components of  $\Delta P_{\text{in}}$ . This is justified by noting that the conduction current density per molecule within a time  $\omega^{-1}$  is the displacement of charge out-of-phase with the real part of the ionic field due to optical conductivity. This out-of-phase charge displacement is alternatively given by the formally defined dipole  $p_{\alpha_2}$ . The dipole  $p_{\alpha_2}$  defined in this way interacts with the permanent and induced moments of the multipole expansion to give inner-sphere energy



losses. In this way, the inner-sphere interaction energies are damped by the optical conduction of the medium. Thus,

$$L_{in} = L(\sigma_{IND}) + L(e\sigma) + L(p\sigma) + L(p_{\alpha}\sigma) + L(q\sigma) + L_{REP} \quad (24)$$

where  $L(\sigma_{IND})$  represents the damping of the induction energy over the interval  $\omega^{-1}$  arising from the optical conductivity of the solvent.

Likewise,  $L(e\sigma)$ ,  $L(p\sigma)$ ,  $L(p_{\alpha}\sigma)$ ,  $L(q,\sigma)$  represent the decrease of the interaction energies (or losses) for the charge, dipole, induced dipole and quadrupole terms of Eqs. (2) to (6), respectively. The quantity  $L(\sigma_{IND})$  is the imaginary contribution from the Born repulsion. This term is included because the minimization of the interaction energies with respect to nuclear coordinates, which leads to Eq. (9), minimizes conductive losses as well. London dispersion is not applicable to the loss calculation, however. One has (cf. Sec. IIB),

$$L(\sigma_{IND}) = (N/2)[\alpha_2(p_{\alpha_1}^2 - p_{\alpha_2}^2) - 2\alpha_1 p_{\alpha_1} p_{\alpha_2}]/(\alpha_1^2 + \alpha_2)^2 \quad (25)$$

$$L(e\sigma) = (N/2)(e/r_0^2)p_{\alpha_2} \quad (26)$$

$$L(p\sigma) = -2A(pp_{\alpha_2}/r_0^3)\cos \beta \quad (27)$$

$$L(p_{\alpha}\sigma) = -2Ap_{\alpha_1}p_{\alpha_2}/r_0^3 \quad (28)$$

$$L(q\sigma) = B\theta p_{\alpha_2}/r_0^4 \quad (29)$$

$$L_{REP} = (1/x)\{2L(e\sigma) + 3[L(p\sigma) + L(p_{\alpha}\sigma)] + 4L(q\sigma)\} \quad (30)$$

where  $p_{\alpha_2}$  and the quantities  $A$ ,  $B$ ,  $p$ ,  $\theta$ ,  $x$  are defined in Sec. IIB.

#### IV. TOTAL ENERGY FOR NONEQUILIBRIUM PROCESSES

The total contribution  $W$  from nonequilibrium processes to the exclusion of nuclear reorganization will be obtained. The real and imaginary components of  $W$  are

$$P = \Delta P_{in} + \Delta P_{out} \quad (31)$$

$$L = L_{in} + L_{out} \quad (32)$$

Thus,

$$W = (P^2 + L^2)^{1/2} \quad (33)$$

The variations of  $\Delta P_{in}$ ,  $\Delta P_{out}$ ,  $L_{in}$ ,  $L_{out}$  and  $W$  with photon energy for  $S = 1$  are displayed in Fig. 1 for liquid water for octahedral coordination of the solvent around an anion. The shapes of the curves of Fig. 1 are determined by dielectric dispersion and the absorption bands of liquid water at ca. 8.2 and 10.0 eV. This point is amplified in Sec. V and VI. Results for tetrahedral coordination around an anion are the same except that  $\Delta P_{in}$  makes a contribution to  $W$  which is ca. 18 percent lower than in Fig. 1. Results for cations are similar to those for anions for the same coordination.

Data on  $\epsilon_1$  and  $\epsilon_2$  used in Fig. 1 were those recently recalculated by Painter<sup>23</sup> from earlier results<sup>24-26</sup> on reflectance spectroscopy of liquid water except for  $\epsilon_2$ . The earlier<sup>24</sup> values of  $\epsilon_2$  in the 6.8 to 8.8 eV interval were used because the cut-off  $\epsilon_2 = 0$  below 7.6 eV in Refs. 25 and 26 does not agree with the data from other workers summarized in Ref. 27. The difference is really minor in the calculation of  $L$  but not in that of the derivative  $dL/dE$  needed for comparison with experiment. The quadrupole moment components used in the preparation of Fig. 1 were taken from Ref. 28.

The effect of screening by the ionic atmosphere on the variations of the energy  $W$  of Eq. (33) with the photon energy  $E$  is shown in Fig. 2 for  $S = 0.3$  to  $S = -0.1$ . The shape of the  $W$  against  $E$  curve hardly changes between  $S = 1$  and 0.3, but  $W$  at a given  $E$  decreases with increasing screening. Figure 2, in fact, shows that screening can drastically reduce the magnitude of  $W$ . Whereas the outer-sphere contributions  $\Delta P_{out}$  and  $L_{out}$  become dominant for  $S \gtrsim 0.2$ , one has only  $W = (\Delta P_{in}^2 + L_{in}^2)^{1/2}$  for the case of  $S = 0$ . Negative  $S$  values even further reduce  $W$  since the inner-sphere response is decreased by counterion penetration (Sec. IIC).

## V. CALCULATED DISPERSION SPECTRA

The present theory was tested experimentally by using data<sup>1,2</sup> on photoelectron emission by aqueous solutions of inorganic anions and cations in the 7 to 10.4 eV range of photon energy. Verification of the theory requires plots of  $-dW/dE$  against the photon energy  $E$ . This will be shown first. The emission yield  $Y$  in emission experiments is defined as the number of collected photoelectrons per incident photon. One has  $Y = K(E - E_t)^p$ , where  $E$  is the photon energy,  $E_t$  the threshold energy,  $K$  a quantity independent of  $E$  and  $p = 2, 5/2$  or  $3$  depending<sup>6</sup> on the range of  $E$ . A quadratic dependence was found suitable<sup>1,2</sup> and, in any event, conclusions to be drawn below are essentially unaffected by the choice of exponent.<sup>1</sup> One has in view of the form of the emission law for  $Y$ ,

$$dY^{1/2}/dE = K(1 - dE_t/dE) \quad (34)$$

The threshold energy  $E_t$  is given by<sup>29,30</sup>

$$E_t = \Delta G_{\text{cycle}} + R + W, \quad (35)$$

where  $\Delta G_{\text{cycle}}$  can be written in explicit form for a thermodynamic cycle involving the initial and final states of the emission process (including the surface potential contribution), and  $R$  is the free energy for nuclear reorganization. The quantities  $\Delta G_{\text{cycle}}$  and  $R$  are not affected by dielectric dispersion and are independent of  $E$ . One obtains from Eqs. (34) and (35)

$$dY^{1/2}/dE = K[1 - dW/dE]. \quad (36)$$

It follows from Eq. (36) that the derivatives  $dY^{1/2}/dE$  and  $-dW/dE$  should have the same functional dependence on photon energy. The curves representing the variations of  $dY^{1/2}/dE$  and  $-dW/dE$  with  $E$  will be referred to, respectively, as the experimental and theoretical dispersion spectra.

From Eq. (33)

$$dW/dE = [P/(P^2 + L^2)^{1/2}]dP/dE + [L/(P^2 + L^2)^{1/2}]dL/dE. \quad (37)$$

The two terms on the r.h.s. of Eq. (37) were computed as functions of photon energy by using binomial smoothing filters<sup>31</sup> to obtain the derivatives  $dP/dE$  and  $dL/dE$ . This method is preferable to the use of the Savitsky-Golay convolutes previously used<sup>1,32</sup> to calculate the derivatives. It should be noted in this respect that the data on  $\epsilon_1$  and  $\epsilon_2$  of liquid water from Ref. 23 used in the preparation of Fig. 1 were available at 0.2 eV intervals and were interpolated by means of quadratic and quartic polynomials. Interpolation was of no consequence in the calculation of the curves of Fig. 1 but resulted in the elimination or at least damping of any fine structure the derivative curves might actually have in the 0.2 eV intervals. Figure 3 shows that the terms in  $dP/dE$  and  $dL/dE$  in Eq. (37) make comparable contributions to  $-dW/dE$  but that their extrema occur at different photon energies.

The use of the corrected Lorenz-Lorentz equation<sup>21</sup> increases the magnitude of  $|-dW/dt|$  by ca. 10 percent but does not change the functional dependence of  $-dW/dt$  on photon energy.

The difference in the orientation of the water molecules in the inner-sphere shell around anions and cations (Sec. IIB) was investigated. Calculated dispersion spectra for cations exhibit practically the same functional dependence on photon energy as anions but the amplitude is increased, e.g., by ca. 50 percent in comparison with Fig. 3 for the following data:  $N = 6$ ,  $r_c = 0.88 \text{ \AA}$ ,  $\beta = 0$ ,  $\alpha = 1.3 \times 10^{-24} \text{ cm}^3$ ,  $I_s = 26.4 \text{ eV}$ ,  $x = 8$  (data corresponding to the nonhydrated  $V^{2+}$  in Ref. 8).

The effect of screening by the ionic atmosphere is displayed in Fig. 4. The shape of the dispersion spectrum curve is not sensitive to screening between  $S = 1$  and  $S = 0.2$ , but a major change in shape occurs at  $S \lesssim 0.2$ . This is the case because the curves corresponding to  $dP/dE$  and  $dL/dE$  peak at different photon energies (Fig. 3). The curve for  $S = 0$  corresponds to the

case in which the dispersion spectrum is solely determined by the inner-sphere contributions. Conversely, the contributions from the outer-sphere region are dominant for  $S = 1$ . The photon energies at the extrema of the dispersion spectra calculated for  $S = 1$  and  $S = 0$  are listed in Table I. The ranges of  $E < 7.75$  eV and  $7.75 < E < 8.70$  eV correspond respectively to normal and anomalous dispersion for the first absorption band of liquid water (with maximum at ca. 8.2 eV). A maximum between the two minima is displayed in the normal range, and conversely a minimum between two maxima is observed in the anomalous range. This pattern of extrema, which will be referred to as inner-outer sphere splitting, is repeated in the normal and anomalous ranges at higher photon energies for the second absorption band of liquid water (ca. 10.0 eV).

#### VI. COMPARISON OF EXPERIMENTAL AND CALCULATED DISPERSION SPECTRA

Experimental and calculated dispersion spectra are compared in Figs. 5 and 6 for 1-1 (NaSCN) and 1-2 ( $\text{Na}_2\text{S}_2\text{O}_3$ ) electrolytes. The ordinate of experimental dispersion spectra is obtained in arbitrary units, and consequently the curves of Figs. 5 and 6 were normalized at the maximum (8.2 to 8.6 eV) and minimum (ca. 9.1 eV) of the experimental curves. The calculated curves were prepared for  $S = 0.3$  and  $0.15$  (Fig. 5) and  $S = 0.0$  and  $-0.1$  (Fig. 6) for the 0.25 and 2 M solutions, respectively. These values of  $S$  are significantly different at high ionic strengths from the ones computed from Eq. (13) with  $\kappa^{-1}$  measured from a: 0.41 (0.25 M) and  $-0.14$  (2 M) for a 1-1 electrolyte; 0.14 (0.25 M) and  $-0.40$  (2 M) for a 1-2 electrolyte. This is not surprising since an accurate calculation of  $\kappa^{-1}$  from the Debye-Hückel theory in its original form, as applied in Eq. (13), is not possible at the concentrations of Figs. 5 and 6.

The experimental curves for the 2 M solution of Figs. 5 and 6 have slightly different widths than the calculated dispersion spectra. Three possible reasons at least can be advanced for this discrepancy: the uncertainty about  $\epsilon_1$  and  $\epsilon_2$  inherent to the application of the Kramers-Kronig transformation in reflectance spectroscopy<sup>33</sup>; the uncertainty about  $\epsilon_2$  below ca. 8.8 eV (Sec. IV); the approximation of the theoretical model in which spherical symmetry of the field is assumed around the ion undergoing photoionization.

The change in the shape of dispersion spectra upon increase of the ionic strength is strikingly apparent in Figs. 5 and 6. Thus, the maximum with dominant outer-sphere contribution near 8.6 eV is prominent for the 0.25 M sodium thiocyanate solution whereas the maximum with dominant inner-sphere contribution near 8.2 eV is considerably enhanced for 2 M thiosulfate. Inner-outer sphere splitting (cf. Table I) in the 8.0 to 8.8 eV and 9.0 to 9.7 eV ranges is indeed observed. Figures 5 and 6 also show that the weak maximum at 9.38 eV in the calculated curves is greatly enhanced in the experimental curves. Inner-outer sphere splitting in the 9.0 to 9.7 eV range therefore can be strongly influenced by the nature of the anion. This specific effect is displayed by the 17 anions studied in Ref. 1. Thus, the height of the 9.37 eV peak is nearly independent of concentration (0.25 to 2 M) for some anions (e.g.,  $\text{OH}^-$ ,  $\text{CO}_3^{2-}$ ,  $\text{SCN}^-$ ) whereas it is strongly concentration-dependent for others (e.g.,  $\text{Br}^-$ ,  $\text{I}^-$ ,  $\text{ClO}_4^-$ ). The 9.63 eV minimum is also sensitive to the nature of the anions as is evident from Figs. 5 and 6. Particularly pronounced minima were observed in Ref. 1 with bromide at 9.62 eV and iodide at 9.59 eV. Greatly enhanced inner-outer sphere splitting was recently observed for phosphorus hexafluoride ion (0.2 M  $\text{KPF}_6$ ,  $E_t \sim 9.3$  eV) with the normal sequence of two maxima (10.02 and 10.35 eV) and a minimum

(10.18 eV). This enhancement from  $\text{PF}_6^-$  ion completely masked the dispersion spectrum of liquid water ( $E_t = 10.06$  eV).

The photon energies at the extrema of the experimental dispersion spectra of the 17 anions studied in Ref. 1 in Table I compare very well with the calculated values for  $-0.2 \leq S \leq 1$ . It is concluded from this agreement and the interpretation in Sec. V and VI that the theory accounts remarkably well for the experimental dispersion spectra and the pronounced effect of ionic strength on their shape.

The present theory is supported also by the observed shift in threshold energy with concentration of ionic emitter for  $\text{NaSCN}$ ,  $\text{NaN}_3$ ,  $\text{Na}_2\text{S}_2\text{O}_3$  and  $\text{Na}_2\text{S}_2\text{O}_8$  over the 0.25 to 2.0 M range. Further work on this aspect will be the subject of a future publication.

## VII. CONCLUSIONS

Photoionization provides a way of changing the intense ionic field in a time interval corresponding to the frequency of the incident radiation. These rapid variations of the ionic field can be used to probe the response of liquids and solutions. Experimental evidence was obtained in this way for nonequilibrium electronic processes resulting from dielectric dispersion of the solvent in photoionization. Theory predicts and experiment confirms that ionic screening can alter profoundly the balance between the contributions from inner- and outer-sphere regions to the energetics of the nonequilibrium electronic processes (inner-outer sphere splitting).

## ACKNOWLEDGMENTS

This work was supported by the Office of Naval Research and the National Science Foundation. We thank Professor N. S. Hush (Theoretical Chemistry, Sydney) for pointing out to us the need to consider the difference in solvent configuration around inorganic anions and cations. Professor L. R. Painter

(Physics, University of Tennessee) kindly communicated her unpublished recalculated data on the reflectance spectroscopy of liquid water.

## APPENDIX

### A. Quadrupole moment

The quadrupole moment of Eq. (6) for  $\beta = 0$  is<sup>9</sup>

$$\Theta = \Theta_a + \Theta_b \quad (A1)$$

where

$$\Theta_a + \Theta_b = 2\Theta_{zz} - \Theta_{xx} - \Theta_{yy}, \quad (A2)$$

the z-axis being in the ion-oxygen direction. For  $\beta = 52.23^\circ$ , one has

$$\Theta_a + \Theta_b = 2\Theta_{zz}\sec\beta - \Theta_{xx}\sec\beta - \Theta_{yy}. \quad (A3)$$

Equation (A3) was obtained by noting that the water molecule rotates about the H-O axis for  $\beta = 52.23^\circ$ . The quantities  $\Theta_a$  and  $\Theta_b$  therefore were transformed with respect to the new axis of rotation.

### B. Attenuation of the field

The electric field in a conducting, isotropic medium is attenuated<sup>34</sup> by the factor  $\exp(-\omega kr/c)$ , where  $k$  is the absorption coefficient,  $r$  the depth of penetration and  $c$  the velocity of light in vacuum. The absorption coefficient  $k$  can be computed from  $\epsilon_1 = n^2 - k^2$  and  $\epsilon_2 = 2nk$ , where  $n$  is the index of refraction. The field in the present case is proportional to  $r^{-2}$  without attenuation. The energy without attenuation is obtained by integrating  $r^{-4}dV$  from  $a$  to  $\infty$ , where  $dV = 4\pi r^2 dr$ . With attenuation, one integrates  $4\pi r^{-2}\exp(-2\omega kr/c)dr$  between  $a$  and  $\infty$ . This is done in the calculation of  $\Delta P_{out}$  using the real part of  $(\epsilon_1 - i\epsilon_2)^{-1}$  as noted in Sec. III. There is no attenuation of the field for the limiting value  $\epsilon_{op}^0$ . One obtains

$$\begin{aligned} \Delta P_{out} = & (e^2/2a)(\epsilon_{op}^0)^{-1} - (e^2/2)\epsilon_1(\epsilon_1^2 + \epsilon_2^2)^{-1}[a^{-1}\exp(-\xi a) \\ & + \xi \ln \xi a - \xi^2 a + \xi^3/2.2! \dots], \end{aligned} \quad (A4)$$

where  $\xi = 2\omega k/c$ . The series in (A4) converges rapidly in the present case and



only the first term between brackets is significant. Equation (A4) reduces to Eq. (11) for  $\xi = 0$ . One has<sup>23</sup> for liquid water at 8.2 eV,  $k = 0.19$ ,  $\xi = 7.5 \times 10^{-3} \text{ cm}^{-1}$  and  $\exp(-\xi a) = 0.992$ . Attenuation of the field thus changes the second term on the r.h.s. of Eq. (A4) by only  $\approx 1$  percent.

## REFERENCES

- <sup>1</sup>P. Delahay and A. Dziedzic, J. Chem. Phys. 80, 5381 (1984).
- <sup>2</sup>P. Delahay and A. Dziedzic, J. Chem. Phys. 81, 3678 (1984).
- <sup>3</sup>N. S. Hush, private communication.
- <sup>4</sup>C. N. Berglund and W. E. Spicer, Phys. Rev. 136A, 1030, 1044 (1964).
- <sup>5</sup>A. M. Brodsky and A. V. Tsarevsky, J. Chem. Soc. Faraday Trans. 2, 72, 1781 (1976).
- <sup>6</sup>A. M. Brodsky, J. Phys. Chem. 84, 1856 (1980).
- <sup>7</sup>A. D. Buckingham, Disc. Faraday Soc. 24, 151 (1957).
- <sup>8</sup>W. E. Morf and W. Simon, Helv. Chim. Acta 54, 794 (1971).
- <sup>9</sup>R. A. Marcus, J. Chem. Phys. 24, 966, 979 (1956).
- <sup>10</sup>N. S. Hush, Trans. Faraday Soc. 57, 557 (1961).
- <sup>11</sup>H. Margenau and N. R. Kestner, Theory of Intermolecular Forces (Pergamon, London, 1969), p. 17.
- <sup>12</sup>I. G. John, G. B. Bacskay, and N. S. Hush, Chem. Phys. 51, 49 (1980).
- <sup>13</sup>P. Schuster, in Electron-Solvent and Anion-Solvent Interactions, L. Kevan and B. C. Webster, eds. (Elsevier, Amsterdam, 1976), pp. 264, 289-291.
- <sup>14</sup>E. A. Moelwyn-Hughes, Physical Chemistry, 2nd ed. (Pergamon, London, 1961), pp. 308-309.
- <sup>15</sup>J. E. Enderby and G. W. Neilson, in Water, vol. 6, F. Franks, ed. (Plenum, New York, 1979), pp. 1-46.
- <sup>16</sup>J. E. Enderby and G. W. Neilson, Rep. Progr. Phys. 44, 594 (1981).
- <sup>17</sup>J. E. Enderby, Ann. Rev. Phys. Chem. 34, 155 (1983).

- <sup>18</sup>R. A. Robinson and R. H. Stokes, Electrolyte Solutions (Butterworths, London, 1959), pp. 218-220, 228-229, 236-238, 491-503.
- <sup>19</sup>E. Waisman, G. Worry, and R. A. Marcus, J. Electroanal. Chem. 82, 9 (1977).
- <sup>20</sup>B. A. Pailthorpe, D. J. Mitchell, and B. W. Ninham, J. Chem. Soc. Faraday Trans. 2, 80, 115 (1984).
- <sup>21</sup>C. J. F. Böttcher and P. Bordewijk, Theory of Electric Polarization, vol. II, 2nd ed. (Elsevier, Amsterdam, 1978), pp. 23-27, 292-301, 395-404.
- <sup>22</sup>Y. Aharonov and A. Petersen, in Quantum Theory and Beyond (University Press, Cambridge, 1971), pp. 135-139.
- <sup>23</sup>L. R. Painter, private communication.
- <sup>24</sup>L. R. Painter, R. D. Birkhoff, and E. T. Arakawa, J. Chem. Phys. 51, 243 (1969).
- <sup>25</sup>J. M. Heller, Jr., R. N. Hamm, R. D. Birkhoff, and L. R. Painter, J. Chem. Phys. 60, 3483 (1978).
- <sup>26</sup>J. M. Heller, Jr., R. D. Birkhoff, and L. R. Painter, J. Chem. Phys. 67, 1858 (1977).
- <sup>27</sup>F. Williams, S. P. Varma, and S. Hillenius, J. Chem. Phys. 64, 1549 (1976).
- <sup>28</sup>J. Verhoeven and A. Dymanus, J. Chem. Phys. 52, 3222 (1970).
- <sup>29</sup>P. Delahay, in Electron Spectroscopy: Theory, Techniques and Applications, vol. 5, C. R. Brundle and A. D. Baker, eds. (Academic Press, London, 1984), pp. 123-196.
- <sup>30</sup>P. Delahay and A. Dziedzic, J. Chem. Phys. 80, 5793 (1984).
- <sup>31</sup>P. Marchand and L. Marmet, Rev. Sci. Instrum. 54, 1034 (1982).
- <sup>32</sup>A. Dziedzic, "Energetics and Dispersion of Optical Electron Transfer in Solution," Ph.D. dissertation, New York University, 1984.
- <sup>33</sup>R. H. Young, J. Opt. Soc. Am. 67, 520 (1977).
- <sup>34</sup>J. D. Jackson, Classical Electrodynamics, 2nd ed. (Wiley, New York, 1975), pp. 296-298.

TABLE I. Photon energies at the extrema of experimental and calculated dispersion spectra ( $S = 0$  and 1)

| Dispersion                          | Extremum | Dominant Contribution | Calculated <sup>a</sup><br>Photon Energy<br>(eV) | Experimental <sup>b</sup><br>Photon Energy<br>(eV) |
|-------------------------------------|----------|-----------------------|--|--|
| normal<br>( $< 7.75$ eV)            | min      | inner                 | 7.24   | no datum   |
|                                     | max      | mixed                 | 7.30   | 7.30   |
|                                     | min      | outer                 | 7.42   | 7.41   |
| anomalous<br>( $7.75$ to $8.70$ eV) | max      | inner                 | 8.24   | $8.16 \pm 0.06$                                    |
|                                     | min      | mixed                 | 8.58   | $8.42 \pm 0.06$                                    |
|                                     | max      | outer                 | 8.68   | $8.65 \pm 0.03$                                    |
| normal<br>( $8.70$ to $9.70$ eV)    | min      | inner                 | 9.18   | $9.11 \pm 0.03$                                    |
|                                     | max      | mixed                 | 9.38   | $9.37 \pm 0.06$                                    |
|                                     | min      | outer                 | 9.63   | $9.63 \pm 0.12$                                    |
| anomalous<br>( $> 9.7$ eV)          | max      | inner                 | 9.96   | $9.86 \pm 0.04$                                    |
|                                     | min      | mixed                 | 10.11  | 10.18  |
|                                     | max      | outer                 | 10.32  | 10.35  |

<sup>a</sup>See Fig. 4 for  $7 \leq E \leq 10$  eV.

<sup>b</sup>Data for  $0.5$  M  $\text{VCl}_2$  and  $1$  M  $\text{CrCl}_2$  ( $7.30$  and  $7.41$  eV) and  $0.05$  M  $\text{K}_4\text{Fe}(\text{CN})_6$  ( $7.41$  eV) from Ref. 2. Average values with standard deviation ( $8.16 \leq E \leq 10$  eV) for  $1$  M solutions of 17 inorganic anions from Ref. 1. Extrema at  $10.18$  and  $10.35$  eV obtained with  $0.2$  M  $\text{KPF}_6$ .

## Captions to Figures

Fig. 1 Variation of energies with photon energy for liquid water and the solvent configuration around a typical inorganic anion:  $\Delta P_{in}$ ,  $L_{in}$  and  $\Delta P_{out}$ ,  $L_{out}$  for the inner- and outer-sphere regions, respectively,  $W$  the total energy from Eq. (25). Data:  $N = 6$ ,  $r_c = 2 \text{ \AA}$ ,  $r_w = 1.38 \text{ \AA}$ ,  $\beta = 52.23^\circ$ ,  $p = 1.855 \text{ debye}$ ,  $\alpha^0 = 1.444 \times 10^{-24} \text{ cm}^3$ ,  $\alpha_s = 4 \times 10^{-24} \text{ cm}^3$ ,  $I_s = 3 \text{ eV}$ ,  $I = 12.61 \text{ eV}$ ,  $x = 12$ . Values of  $\epsilon_1$  and  $\epsilon_2$  from Ref. 23 (see text). No screening by the ionic atmosphere ( $S = 1$ ).

Fig. 2. Variations of the total energy  $W$  with photon energy for different values of the screening factor  $S$  ( $S = 0$  for complete outer-sphere screening,  $S = -0.1$  for partial screening of the inner-sphere). Same data as in Fig. 1.

Fig. 3. Variations of the quantities in Eq. (29) with photon energy for the data of Fig. 1.

Fig. 4. Variations of  $-dW/dE$  with photon energy for different values of the screening factor  $S$  ( $S = 0$  for complete screening of the outer-sphere,  $S = -0.1$  for partial screening of the inner-sphere). Same data as in Fig. 1.

Ordinates at the minimum at 7.42 eV from  $S = -0.1$  to  $S = 1.0$ : -0.164, -0.196, -0.229, -0.263, -0.297, -0.541. Ordinates at the maximum (photon energy between parentheses) from  $S = -0.1$  to  $S = 1.0$ : 0.151 (8.20 eV), 0.151 (8.24 eV), 0.162 (8.35 eV), 0.181 (8.41 eV), 0.216 (8.68 eV), 0.509 (8.68 eV).

Fig. 5. Comparison of experimental dispersion spectra for 0.25 M (bottom) and 2 M sodium thiocyanate with dispersion spectra calculated for the data of Fig. 1 and a screening factor  $S = 0.3$  (bottom) and 0.15 (top).

Fig. 6. Same comparison as in Fig. 5 but for 0.25 M (bottom) and 2 M sodium thiosulfate and  $S = 0.0$  (bottom) and -0.1 (top).

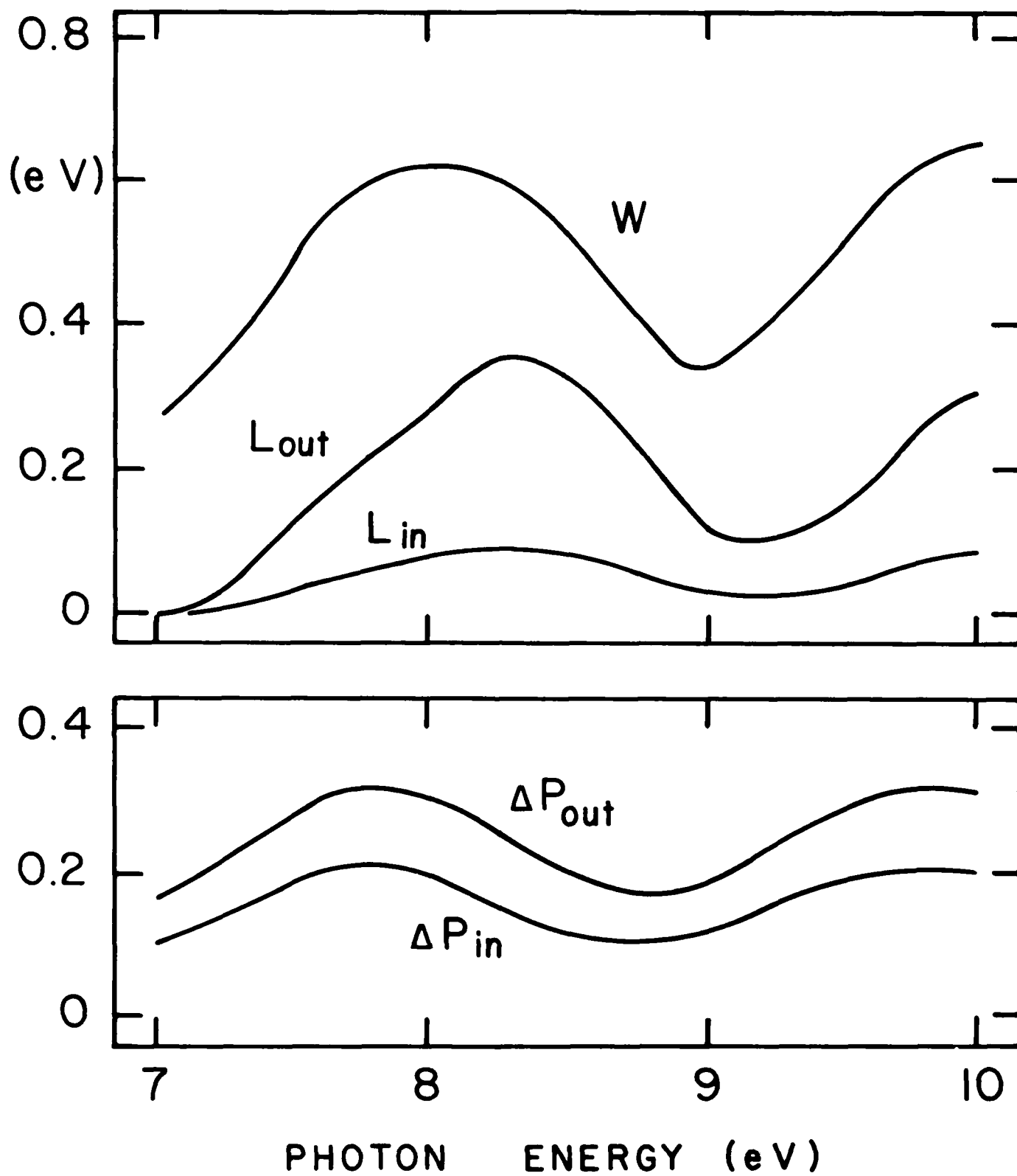


FIG. 1

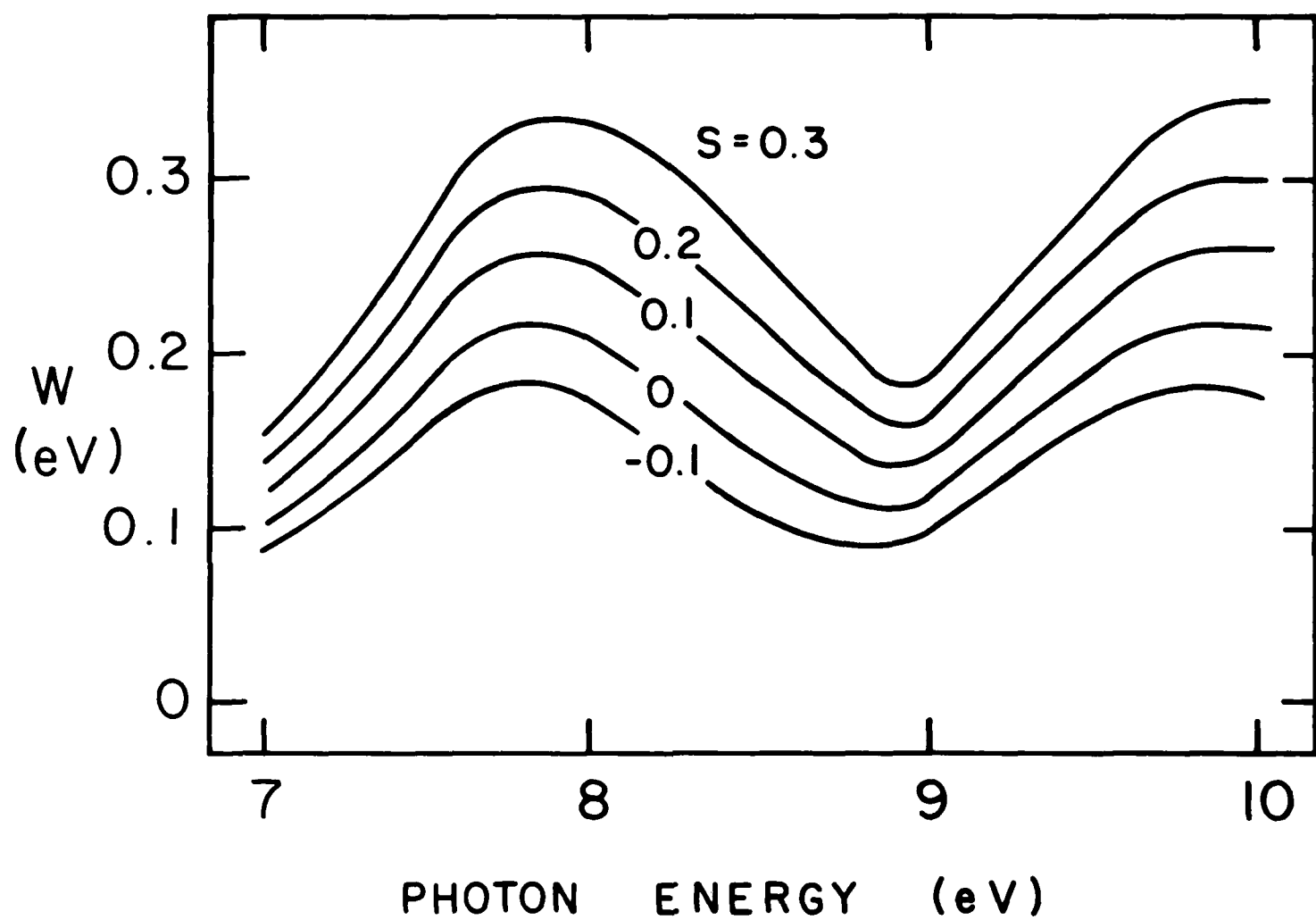


FIG. 2

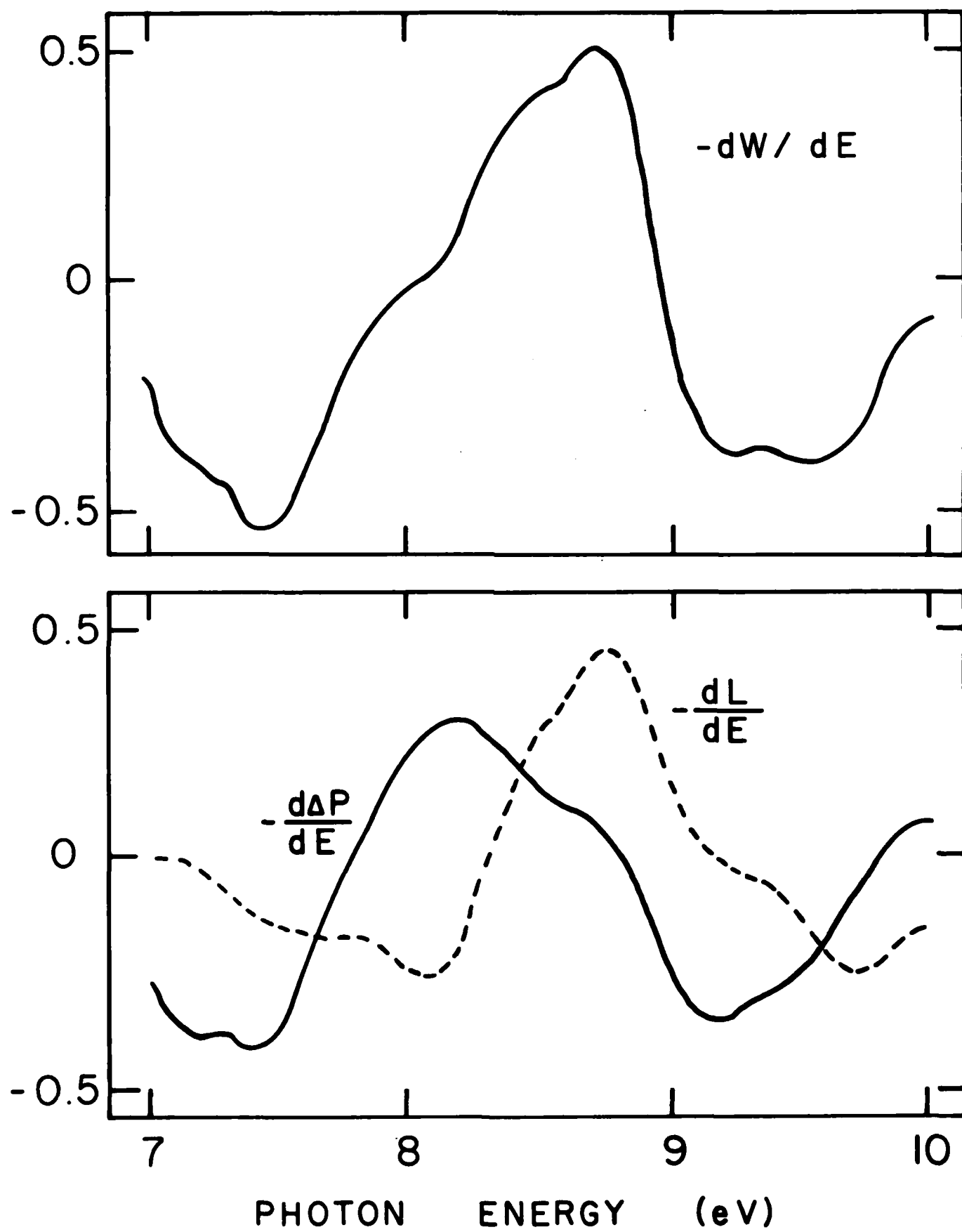


FIG. 3

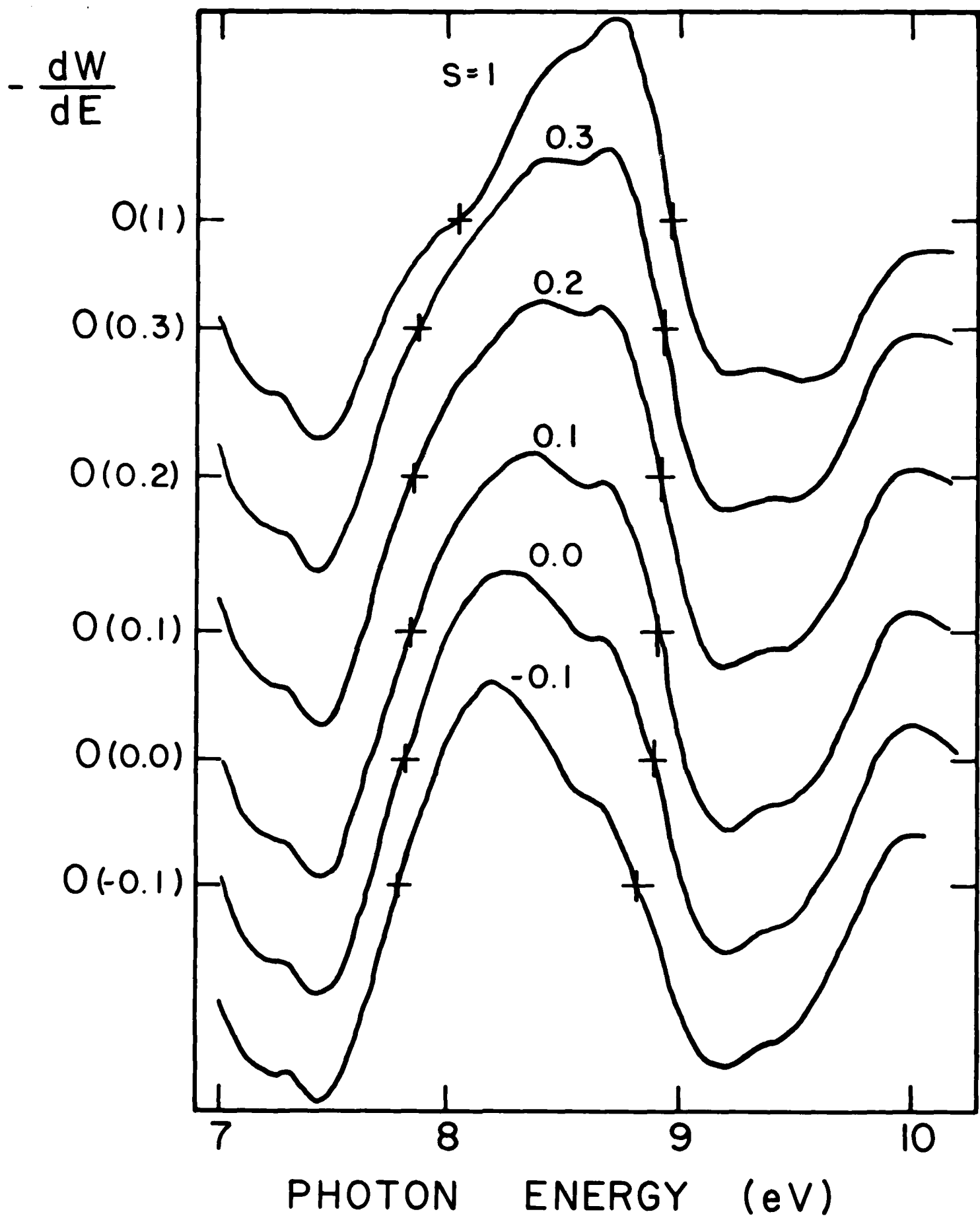


FIG. 4



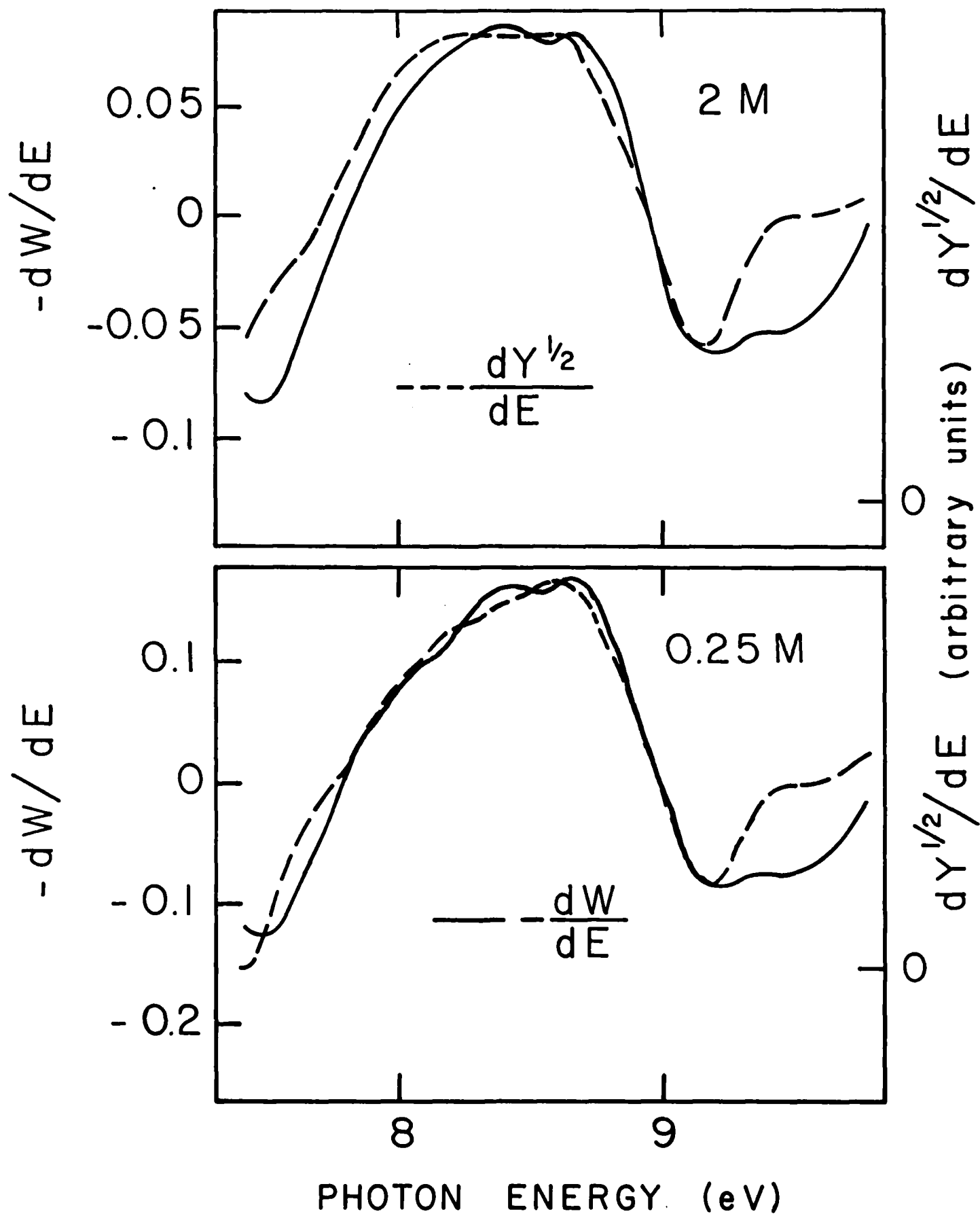


FIG. 5

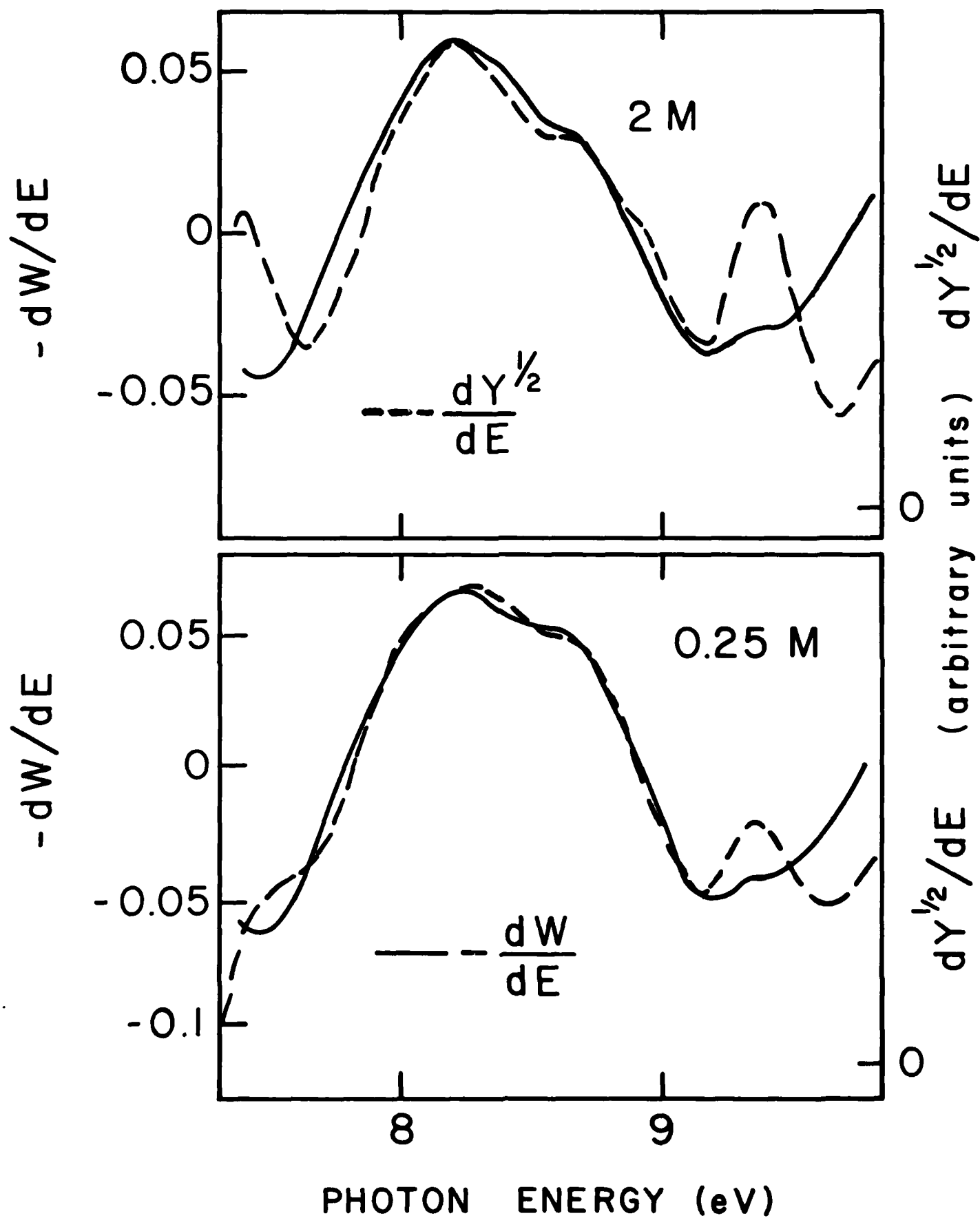


FIG. 6

TECHNICAL REPORT DISTRIBUTION LIST, GEN

|  | <u>No.<br/>Copies</u> |  | <u>No.<br/>Copies</u> |
|--|-----------------------|--|-----------------------|
| Office of Naval Research<br>Attn: Code 413<br>800 N. Quincy Street<br>Arlington, Virginia 22217                              | 2                     | Dr. David Young<br>Code 334<br>NORDA<br>NSTL, Mississippi 39529  | 1                     |
| Dr. Bernard Douda<br>Naval Weapons Support Center<br>Code 5042<br>Crane, Indiana 47522                                       | 1                     | Naval Weapons Center<br>Attn: Dr. A. B. Amster<br>Chemistry Division<br>China Lake, California 93555           | 1                     |
| Commander, Naval Air Systems<br>Command<br>Attn: Code 310C (H. Rosenwasser)<br>Washington, D.C. 20360                        | 1                     | Scientific Advisor<br>Commandant of the Marine Corps<br>Code RD-1<br>Washington, D.C. 20380                    | 1                     |
| Naval Civil Engineering Laboratory<br>Attn: Dr. R. W. Drisko<br>Port Hueneme, California 93401                               | 1                     | U.S. Army Research Office<br>Attn: CRD-AA-IP<br>P.O. Box 12211<br>Research Triangle Park, NC 27709             | 1                     |
| Defense Technical Information Center<br>Building 5, Cameron Station<br>Alexandria, Virginia 22314                            | 12                    | Mr. John Boyle<br>Materials Branch<br>Naval Ship Engineering Center<br>Philadelphia, Pennsylvania 19112        | 1                     |
| DTNSRDC<br>Attn: Dr. G. Bosmajian<br>Applied Chemistry Division<br>Annapolis, Maryland 21401                                 | 1                     | Naval Ocean Systems Center<br>Attn: Dr. S. Yamamoto<br>Marine Sciences Division<br>San Diego, California 91232 | 1                     |
| Dr. William Tolles<br>Superintendent<br>Chemistry Division, Code 6100<br>Naval Research Laboratory<br>Washington, D.C. 20375 | 1                     |  |                       |

ABSTRACTS DISTRIBUTION LIST, 359/627

Dr. Paul Delahay  
Department of Chemistry  
New York University  
New York, New York 10003

Dr. P. J. Hendra  
Department of Chemistry  
University of Southampton  
Southampton SO9 5NH  
United Kingdom

Dr. T. Katan  
Lockheed Missiles and  
Space Co., Inc.  
P.O. Box 504  
Sunnyvale, California 94088

Dr. D. N. Bennion  
Department of Chemical Engineering  
Brigham Young University  
Provo, Utah 84602

Mr. Joseph McCartney  
Code 7121  
Naval Ocean Systems Center  
San Diego, California 92152

Dr. J. J. Auburn  
Bell Laboratories  
Murray Hill, New Jersey 07974

Dr. Joseph Singer, Code 302-1  
NASA-Lewis  
21000 Brookpark Road  
Cleveland, Ohio 44135

Dr. P. P. Schmidt  
Department of Chemistry  
Oakland University  
Rochester, Michigan 48063

Dr. H. Richtol  
Chemistry Department  
Rensselaer Polytechnic Institute  
Troy, New York 12181

Dr. R. A. Marcus  
Department of Chemistry  
California Institute of Technology  
Pasadena, California 91125

Dr. E. Yeager  
Department of Chemistry  
Case Western Reserve University  
Cleveland, Ohio 44106

Dr. C. E. Mueller  
The Electrochemistry Branch  
Naval Surface Weapons Center  
White Oak Laboratory  
Silver Spring, Maryland 20910

Dr. Sam Perone  
Chemistry & Materials  
Science Department  
Lawrence Livermore National Laboratory  
Livermore, California 94550

Dr. Royce W. Murray  
Department of Chemistry  
University of North Carolina  
Chapel Hill, North Carolina 27514

Dr. B. Brummer  
EIC Incorporated  
111 Downey Street  
Norwood, Massachusetts 02062

Dr. Adam Heller  
Bell Laboratories  
Murray Hill, New Jersey 07974

Electrochimica Corporation  
Attn: Technical Library  
2485 Charleston Road  
Mountain View, California 94040

Library  
Duracell, Inc.  
Burlington, Massachusetts 01803

Dr. A. B. Ellis  
Chemistry Department  
University of Wisconsin  
Madison, Wisconsin 53706

Dr. Manfred Breiter  
Institut für Technische Elektrochemie  
Technischen Universität Wien  
9 Getreidemarkt, 1160 Wien  
AUSTRIA

ABSTRACTS DISTRIBUTION LIST, 359/627

Dr. M. Wrighton  
Chemistry Department  
Massachusetts Institute  
of Technology  
Cambridge, Massachusetts 02139

Dr. B. Stanley Pons  
Department of Chemistry  
University of Utah  
Salt Lake City, Utah 84112

Donald E. Mains  
Naval Weapons Support Center  
Electrochemical Power Sources Division  
Crane, Indiana 47522

S. Ruby  
DOE (STOR)  
M.S. 6B025 Forrestal Bldg.  
Washington, D.C. 20595

Dr. A. J. Bard  
Department of Chemistry  
University of Texas  
Austin, Texas 78712

Dr. Janet Osteryoung  
Department of Chemistry  
State University of New York  
Buffalo, New York 14214

Dr. Donald W. Ernst  
Naval Surface Weapons Center  
Code R-33  
White Oak Laboratory  
Silver Spring, Maryland 20910

Mr. James R. Moden  
Naval Underwater Systems Center  
Code 3632  
Newport, Rhode Island 02840

Dr. Bernard Spielvogel  
U.S. Army Research Office  
P.O. Box 12211  
Research Triangle Park, NC 27709

Dr. Aaron Fletcher  
Naval Weapons Center  
Code 3852  
China Lake, California 93555

Dr. M. M. Nicholson  
Electronics Research Center  
Rockwell International  
3370 Miraloma Avenue  
Anaheim, California

Dr. Michael J. Weaver  
Department of Chemistry  
Purdue University  
West Lafayette, Indiana 47907

Dr. R. David Rauh  
EIC Laboratories, Inc.  
111 Downey Street  
Norwood, Massachusetts 02062

Dr. Aaron Wold  
Department of Chemistry  
Brown University  
Providence, Rhode Island 02192

Dr. Martin Fleischmann  
Department of Chemistry  
University of Southampton  
Southampton SO9 5NH ENGLAND

Dr. R. A. Osteryoung  
Department of Chemistry  
State University of New York  
Buffalo, New York 14214

Dr. Denton Elliott  
Air Force Office of Scientific  
Research  
Bolling AFB  
Washington, D.C. 20332

Dr. R. Nowak  
Naval Research Laboratory  
Code 6170  
Washington, D.C. 20375

Dr. D. F. Shriver  
Department of Chemistry  
Northwestern University  
Evanston, Illinois 60201

Dr. Boris Cahan  
Department of Chemistry  
Case Western Reserve University  
Cleveland, Ohio 44106

ABSTRACTS DISTRIBUTION LIST, 359/627

Dr. David Aikens  
Chemistry Department  
Rensselaer Polytechnic Institute  
Troy, New York 12181

Dr. A. B. P. Lever  
Chemistry Department  
York University  
Downsview, Ontario M3J1P3

Dr. Stanislaw Szpak  
Naval Ocean Systems Center  
Code 6343, Bayside  
San Diego, California 95152

Dr. Gregory Farrington  
Department of Materials Science  
and Engineering  
University of Pennsylvania  
Philadelphia, Pennsylvania 19104

M. L. Robertson  
Manager, Electrochemical  
and Power Sources Division  
Naval Weapons Support Center  
Crane, Indiana 47522

Dr. T. Marks  
Department of Chemistry  
Northwestern University  
Evanston, Illinois 60201

Dr. Micha Tomkiewicz  
Department of Physics  
Brooklyn College  
Brooklyn, New York 11210

Dr. Lesser Blum  
Department of Physics  
University of Puerto Rico  
Rio Piedras, Puerto Rico 00931

Dr. Joseph Gordon, II  
IBM Corporation  
K33/281  
5600 Cottle Road  
San Jose, California 95193

Dr. Hector D. Abruna  
Department of Chemistry  
Cornell University  
Ithaca, New York 14853

Dr. D. H. Whitmore  
Department of Materials Science  
Northwestern University  
Evanston, Illinois 60201

Dr. Alan Bewick  
Department of Chemistry  
The University of Southampton  
Southampton, SO9 5NH ENGLAND

Dr. E. Anderson  
NAVSEA-56Z33 NC #4  
2541 Jefferson Davis Highway  
Arlington, Virginia 20362

Dr. Bruce Dunn  
Department of Engineering &  
Applied Science  
University of California  
Los Angeles, California 90024

Dr. Elton Cairns  
Energy & Environment Division  
Lawrence Berkeley Laboratory  
University of California  
Berkeley, California 94720

Dr. D. Cipris  
Allied Corporation  
P.O. Box 3000R  
Morristown, New Jersey 07960

Dr. M. Philpott  
IBM Corporation  
5600 Cottle Road  
San Jose, California 95193

Dr. Donald Sandstrom  
Boeing Aerospace Co.  
P.O. Box 3999  
Seattle, Washington 98124

Dr. Carl Kannewurf  
Department of Electrical Engineering  
and Computer Science  
Northwestern University  
Evanston, Illinois 60201

Dr. Richard Pollard  
Department of Chemical Engineering  
University of Houston  
4800 Calhoun Blvd.  
Houston, Texas 77004

ABSTRACTS DISTRIBUTION LIST, 359/627

Dr. Robert Somoano  
Jet Propulsion Laboratory  
California Institute of Technology  
Pasadena, California 91103

Dr. Johann A. Joebstl  
USA Mobility Equipment R&D Command  
DRDME-EC  
Fort Belvoir, Virginia 22060

Dr. Judith H. Ambrus  
NASA Headquarters  
M.S. RTS-6  
Washington, D.C. 20546

Dr. Albert R. Landgrebe  
U.S. Department of Energy  
M.S. 6B025 Forrestal Building  
Washington, D.C. 20595

Dr. J. J. Brophy  
Department of Physics  
University of Utah  
Salt Lake City, Utah 84112

Dr. Charles Martin  
Department of Chemistry  
Texas A&M University  
College Station, Texas 77843

Dr. H. Tachikawa  
Department of Chemistry  
Jackson State University  
Jackson, Mississippi 39217

Dr. Theodore Beck  
Electrochemical Technology Corp.  
3935 Leary Way N.W.  
Seattle, Washington 98107

Dr. Farrell Lytle  
Boeing Engineering and  
Construction Engineers  
P.O. Box 3707  
Seattle, Washington 98124

Dr. Robert Gotscholl  
U.S. Department of Energy  
MS G-226  
Washington, D.C. 20545

Dr. Edward Fletcher  
Department of Mechanical Engineering  
University of Minnesota  
Minneapolis, Minnesota 55455

Dr. John Fontanella  
Department of Physics  
U.S. Naval Academy  
Annapolis, Maryland 21402

Dr. Martha Greenblatt  
Department of Chemistry  
Rutgers University  
New Brunswick, New Jersey 08903

Dr. John Wasson  
Syntheco, Inc.  
Rte 6 - Industrial Pike Road  
Gastonia, North Carolina 28052

Dr. Walter Roth  
Department of Physics  
State University of New York  
Albany, New York 12222

Dr. Anthony Sammells  
Eltron Research Inc.  
4260 Westbrook Drive, Suite 111  
Aurora, Illinois 60505

Dr. W. M. Risen  
Department of Chemistry  
Brown University  
Providence, Rhode Island 02192

Dr. C. A. Angell  
Department of Chemistry  
Purdue University  
West Lafayette, Indiana 47907

Dr. Thomas Davis  
Polymer Science and Standards  
Division  
National Bureau of Standards  
Washington, D.C. 20234

Ms. Wendy Parkhurst  
Naval Surface Weapons Center R-33  
Silver Spring, Maryland 20910

**END**

**FILMED**

9-85

**DTIC**